2026 IEEE/SICE International Symposium on System Integration (SII)
January 11-14, 2026. Cancún, México

Design of sidewinding snake robot with Reduced Degree of Freedoms

Takeshi AOKI and Yusuke NAGANO, *Member, IEEE*

***Abstract*— The authors have been researching and developing snake robots that can move over fragile ground. Real desert snakes can move over sand using sidewinding locomotion. To realize this locomotion by a snake robot with three dimensions movements, many active DOFs are required to lift its body segments. In this study, we focus on the regularity of sidewinding locomotion passively and report the design of a new mechanism to lift the body segments in conjunction with active degrees of freedom in the horizontal direction. We explain about analysis of the Snake Robot's Trajectory Planning and Sidewinding Movement.**

I. Introduction

Snakes in nature utilize their elongated bodies to traverse uneven terrain and protruding surfaces, performing various tasks through coiling motions. If these actions could be replicated in robots, it would enable the development of highly versatile robots with simple structures. Many snake robots have been developed to mimic the snake's movement in previous research [1]-[4]. Snake robots utilize the characteristic of snake scales, which are slippery in the direction of body movement but non-slippery in lateral directions to progress forward through serpentine motion.

Desert snakes can move over soft sand using a locomotion method called sidewinding. As shown in Figure 1(a), sidewinding locomotion is a method where the snake lifts its grounded body and continuously moves while floating its body between the ground contact trajectories.

Several snake robots capable of sidewinding locomotion have been developed, and their locomotion principles have been demonstrated through operational experiments [5] [6] [7]. Many robots adopt structures with vertical degree of freedoms (DOFs) to achieve sidewinding locomotion [8] [9]. While this functionality is necessary for lifting its body segments to reduce the friction with the ground, we believe that simply lifting the body segments off the ground requires excessive range of motion and is unnecessary for sidewinding locomotion.

Furthermore, conventional snake robots featured a structure where active DOFs in the horizontal and vertical directions were arranged alternately. This caused the structural members of the body to interfere with each other, significantly limiting the range of motion for the bending DOFs. Consequently, the resulting movement was a serpentine motion

(a) Sidewinder[10]

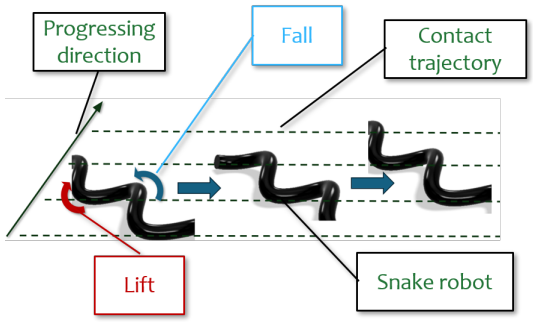

(b) Definition of the locomotion regularity

Figure 1. Sidewinding locomotion: Right turns are ascending and left turns are descending

with small curvature, failing to reproduce the true serpentine curves of a real snake.

Therefore, we focused on the regularity of sidewinding locomotion shown in Fig. 1 (b). In this case, the body is lifted when its body segment is bent to the left and lowered when it is bent to the right to move between contact trajectories. Using this regularity, the snake robot can move its body up and down in conjunction with the lateral bending motion. Since eliminating the active DOFs needed to move the body vertically, a snake robot with reduced DOFs is able to be developed. We have been developing several lifting mechanisms which can lift up the body segments of snake robot by its horizontal motion passively as the previous researches.

In this paper, we propose a new mechanism using crossed helical gears and prototyping of it. We then prototyped a 14-segments snake robot and analyzed its mobility based on the results of performance experiments.

The structure of this paper follows. Section 2 explains the design of body segment with lifting up mechanism using

Takeshi AOKI is with the Chiba Institute of Technology, Tsudanuma 2-17-1, Narashino, Chiba, 275-0016 Japan (e-mail: takeshi.aoki@it-chiba.ac.jp).

Yusuke NAGANO is with the Chiba Institute of Technology, Tsudanuma 2-17-1, Narashino, Chiba, 275-0016 Japan.

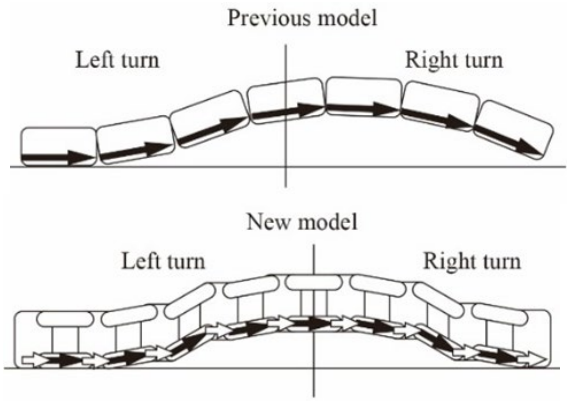

Figure 2. Vector continuity (In the previous model, the vectors don't return to their initial posture)

crossed helical gears. Section 3 describes the prototype model of our snake robot. Section 4 explains the trajectory planning for sidewinding performed by our snake robot. Section 5 discusses the experiments and analysis.

II. Design of Body Segment

A. Problems of previous model

We have developed a lift up mechanism using non-circular gears that constitutes the bending unit as a previous study [11]. The prototype successfully created vertical movement of the fuselage by bending to the left and right horizontally. However, as shown in the upper panel of Fig.2, when the vertical movement of the body segments is considered as a series of vectors, they cannot return to their initial posture because it lands on the ground at a downward angle when it descends. In addition, this cycle is out of phase by 90 degrees when the contact trajectory is viewed as a tangent line between the left and right bends, so it was found that continuous sidewinding locomotion could not be realized with this prototype. Therefore, as shown in Fig.2 lower panel, a mechanism that ensures vector continuity and allows the body segments to move up and down in response to the left-right bending was required.

B. Lift up mechanism

In this study, a new gear mechanism based on the crossed helical gear structure was developed [12]. A mechanism combining a parallel link mechanism was designed to maintain vector continuity. The mechanism is proposed to realize sidewinding locomotion by performing vertical movement of the body segments in conjunction with bending movements to the left and right.

The newly designed lifting mechanism is shown in Fig.3 (a). A pair of crossed helical gear A and B mesh with each other, and their vertical movement is regulated by parallel links. As shown in Fig.3 (b), spur gears are placed above and below the crossed helical gears to propagate the lateral bending angle of the body segment and to constrain the phase of rotation of the crossed helical gears.

By using this mechanism as a unit node, multiple nodes are connected to form a body to realize continuous ascent and

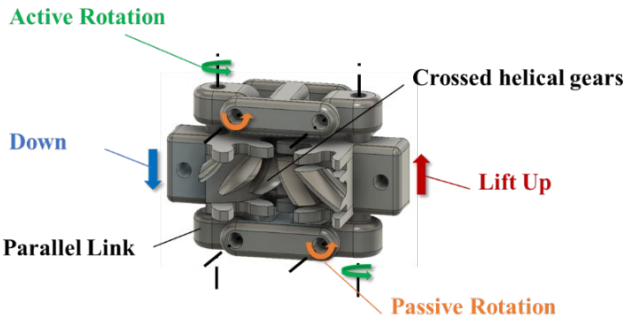

(a) Overview of the lift up mechanism

(b) Horizontal rotation of gears and lifting up synchrony

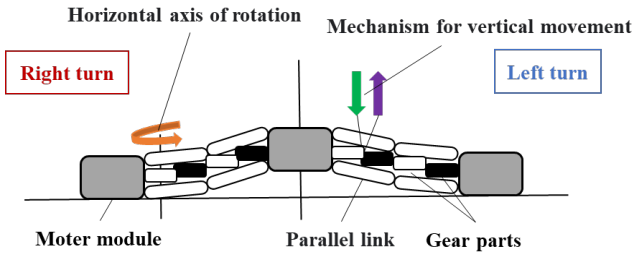

(c) Basic idea of our sidewinding

Figure 3. Lift up mechanism with crossed helical gears

descent in conjunction with horizontal bending, which is necessary for sidewinding locomotion as shown in Fig.3 (c). In addition, because multiple parallel links are continuously connected, there is no problem with vector continuity due to vertical motion. The size of one segment is Height: 23 mm, Width: 35 mm and Length: 24 mm. In this case, the lifting height is small, so the rate of change in the center distance due to the parallel link is 0.2 %, which can be ignored.

C. Lifting up with crossed helical gears

The pair of crossed helical gears in this mechanism meshes the gear A shown in Fig.4 with the gear B shown in Fig.5 that has helical gear teeth arranged on the lift up line. Both gears' helix angle are same and cross section types are transverse.

The lift up line of the gear B always touches with the contact line of the gear A at the contact point between both gears. The lift up line is inclined proportionally to the rotational phase of the spur gear and is arranged as a helix on the pitch circle of the crossed helical gear. The tooth profile of gear B is the involute tooth profile projected onto the lift up line. To prevent interference between the crossed helical gears at the contact points other than those on the lift up line, the tooth shape of gear B is reduced.

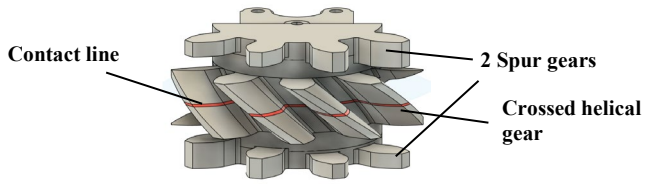

Figure 4. Crossed helical gear A

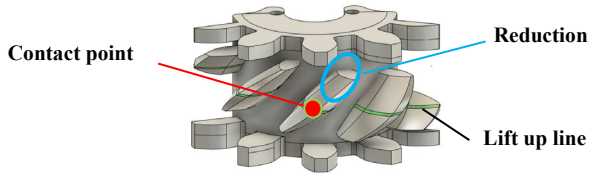

Figure 5. Crossed helical gear B

D. *Lifting up with crossed helical gears*

The pair of crossed helical gears in this mechanism meshes the gear A shown in Fig.4 with the gear B shown in Fig.5 that has helical gear teeth arranged on the lift up line. Both gears' helix angle are same and cross section types are transverse.

The lift up line of the gear B always touches with the contact line of the gear A at the contact point between both gears. The lift up line is inclined proportionally to the rotational phase of the spur gear and is arranged as a helix on the pitch circle of the crossed helical gear. The tooth profile of gear B is the involute tooth profile projected onto the lift up line. To prevent interference between the crossed helical gears at the contact points other than those on the lift up line, the tooth shape of gear B is reduced.

III. PROTOTYPE MODEL

We designed a body segment with a lifting mechanism and prototyped a snake robot by connecting 14 segments. Figure 6 shows the prototype of the sidewinding snake robot. The crossed helical gears constituting the segment has their module changed from 2 to 6. This is to prevent loss of lifting height due to gear backlash. Gear backlash depends not on gear size but on the distance between both gears' shafts. To increase the lifting height while accounting for backlash loss, larger gears are required, necessitating an increase in module size.

As shown in Fig.7, the servo motor is positioned inside the body segment, with the gear A and the gear B arrange at its two ends. The Kondo co. KRS3304ICS servo motor is adopted on our design. Rigidity is enhanced by fixing the parallel link's rotational axis using the bearings of the servo motor's output shaft and the passive shaft on the opposite side of the case. As shown in Fig.7, a structure using parallel links is adopted to connect adjacent unit sections.

The specifications of the new spur gears are shown in Table 1, and the specifications of the new crossed helical gears are shown in Table 2.

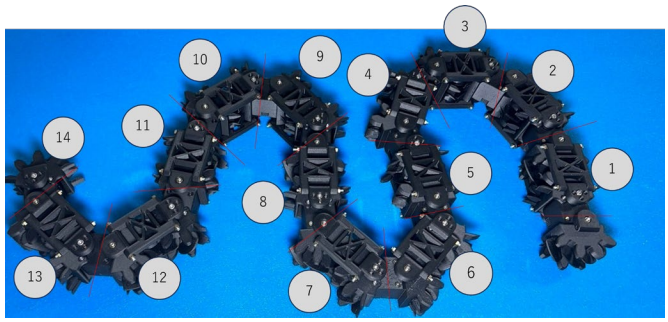

Figure 6. Prototype of sidewinding snake robot. 14 body segments are jointed.

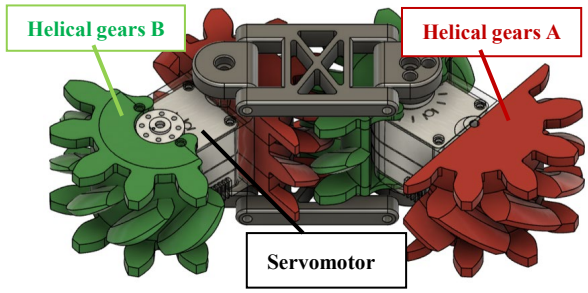

Figure 7. One body segment

TABLE I. SPECIFICATION OF THE SPUR GEARS

Name	Symbol	Formula	First prototype	Second Prototype
Module	M		2.0	6.0
Pressure Angle	α		20°	20°
Number of Teeth	Z	D/M	10	10
Center Distance	a	$(Z_1+Z_2)M/2$	20 [mm]	60[mm]
Pitch circle	D	ZM	20 [mm]	60[mm]

TABLE II. SPECIFICATION OF THE CROSSED HELICAL GEAR

Name	Symbol	Formula	First prototype	Second Prototype
Module	M		2.0	6.0
Pressure Angle	α		20°	20°
Helix Angle	β		35°	35°
Number of Teeth	Z	D/M	10	10
Center Distance	a	$(Z_1+Z_2)M/2$	20[mm]	60[mm]
Pitch circle	D	ZM	20[mm]	60[mm]

Based on the design, a prototype of the actual machine was built. The Markforged 3D printer, the Mark Two, was used for the production. Slicing was performed using Eiger, which is a software exclusive to Markforged. The material used for modeling was onyx, a reinforced nylon resin that is Markforged's proprietary resin material. This resin material is a mixture of nylon and short carbon fibers and is stronger and more dimensionally accurate than nylon. Triangle fill was selected as the infill material. Triangle fill is formed by

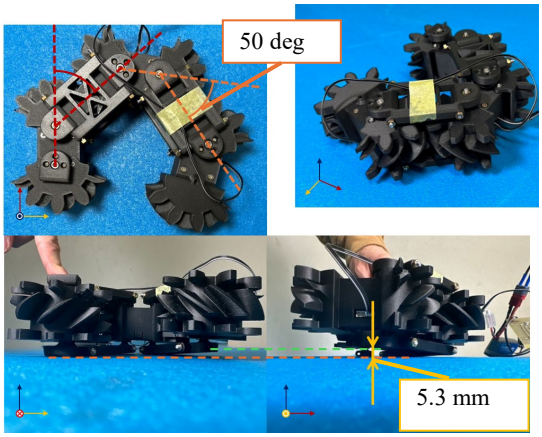

Figure 8. Basic experiment of lifting motion by one segment

stacking equilateral triangles, so it has strength not only in the horizontal direction but also in the vertical direction.

The prototype robot consists of 14 interconnected body segments, with a total length of 1250 mm, width of 72 mm, height of 55 mm, and mass of 850 g. Previously developed snake robots capable of sidewinding were composed of mechanisms where servo motor shafts were arranged by alternating their rotation axes at 90 deg angles [5]-[9]. This design prevented large-angle bending due to link interference. However, our robot is composed of planar double-jointed mechanisms, eliminating actuator interference and enabling a maximum bend angle of 140 deg per one segment. This allows it to replicate the bending angles of a real snake during operation.

An operational experiment was conducted to compare the theoretical and measured values of the lifting height per one segment. The experimental method involved rotating the actuator between segments by 50 deg increments (totaling 100 deg). The lifting height was then measured and compared with the theoretical value, which is 8.3 mm. The experimental results, as shown in Figure 8, confirmed that the active degrees of freedom in the lateral direction propagate to the vertical direction via the crossed helical gear mechanism, causing the one segment to be lifted. The measured result was an elevation of 5.3 mm, falling short of the theoretical value due to factors like backlash. However, this value is enough to achieve sidewinding locomotion.

IV. DESIGN OF SIDEWINDING LOCOMOTION

This section describes the trajectory planning for sidewinding performed by our snake robot. Previous snake robots performed sidewinding by arranging the body trajectory spirally along an elliptical cylinder [7]. However, this method is effective when joint ranges of motion are small and offers few advantages when generating serpentine motion with large bending angles. Therefore, our snake robot uses a different trajectory planning approach.

In our snake robot, the effect of parallel links due to lifting body segments is negligible value, so it is ignored in this study. Therefore, trajectory planning is confined to a two-dimensional plane, with ground contact represented as point contact at the lowest position of a body segment. The meandering curve uses the Serpenoid curve devised by Hirose [13]. The serpinoid curve is a curve where the flexion angle of the body segments changes sinusoidally, closely approximating the undulation of a real snake. In this study, we decided to utilize the advantage of the servo motor's output angle changing smoothly.

The movement of the body segment is represented by $\vec{P}$, consisting of two vectors shown in Equation (1). The contact point with the ground continuously switches along the body, moving along a straight contact trajectory characteristic of sidewinding. The vector moving along this straight trajectory is denoted as $\vec{P}_{ct}$, and the vector moving along a serpentoid curve is denoted as $\vec{P}_{sc}$. The contact point is the transition point where the serpentoid curve changes direction, and the straight line of the contact trajectory becomes the tangent line to the serpentoid curve. The slope of the contact trajectory is the winding angle of the serpentoid curve.

$$\vec{P} = \vec{P}_{ct} + \vec{P}_{sc} = [x_{ct} \quad y_{ct}]^T + [x_{sc} \quad y_{sc}]^T \tag{1}$$

Figure 9 shows one cycle of movement, where v1 is $\vec{P}_{ct}$, v2 is $\vec{P}_{sc}$, and v3 is $\vec{P}$. In this study, to define the serpentoid curve vertically, $\vec{P}_{sc}$ is expressed by equations (2) and (3).

$$x_{sc} = \frac{4l}{\pi}\sum_{m=1}^{\infty}(-1)^{m-1}\frac{J_{2m-1}(\alpha)}{2m-1}\sin\left(\frac{2m-1}{2}\pi\frac{-s}{l}\right) \tag{2}$$

$$y_{sc} = sJ_0(\alpha) - \frac{4l}{\pi}\sum_{m=1}^{\infty}\frac{(-1)^m}{2m}J_{2m}(\alpha)\sin\left(m\pi\frac{-s}{l}\right) \tag{3}$$

Here, l is the length of one-quarter of 1 cycle of the body length, α is the winding angle, s is the length along the snake's body axis, and J(α) is the Bessel function. $\vec{P}_{ct}$ is expressed by equations (4) and (5).

$$x_{ct} = s\sin\alpha \tag{4}$$

$$y_{ct} = s\cos\alpha \tag{5}$$

Figure 10 shows this movement continuously.

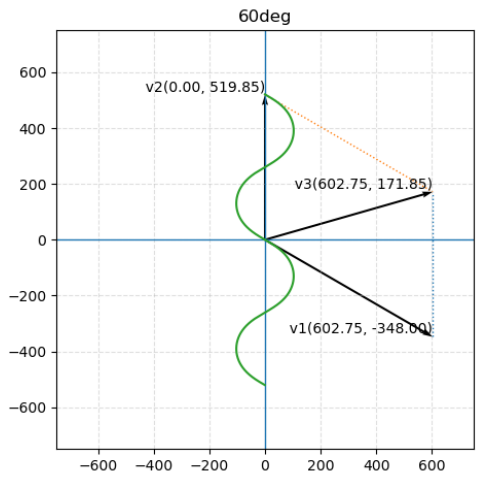

Figure 9. One-cycle movement vector

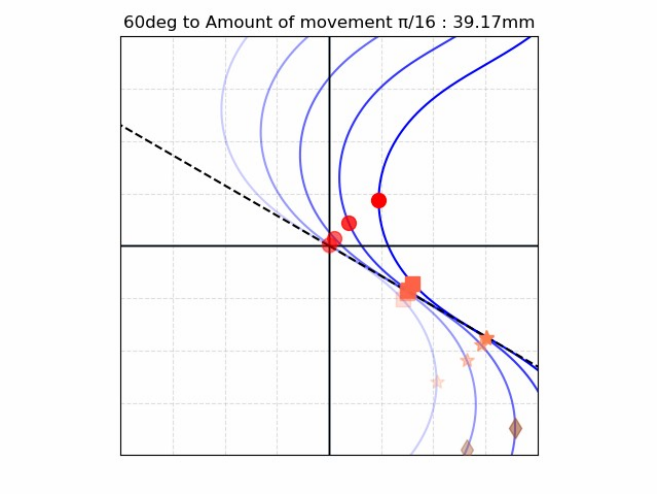

Figure 10. Continuous movement of sidewinding locomotion

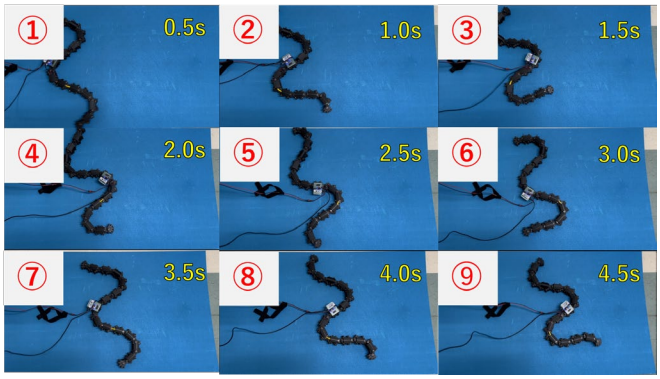

Figure 11. Sidewinding by 60 deg winding angle

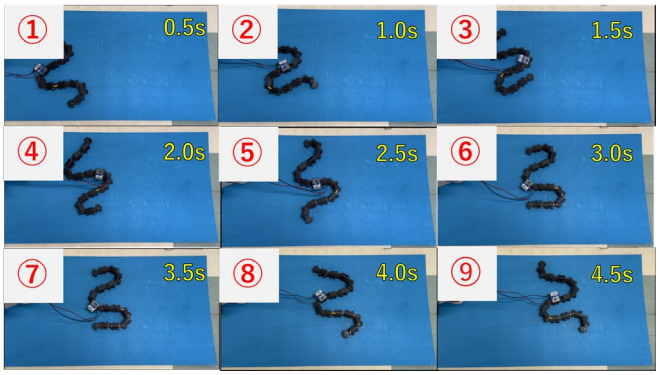

Figure 12. Sidewinding by 90 deg winding angle

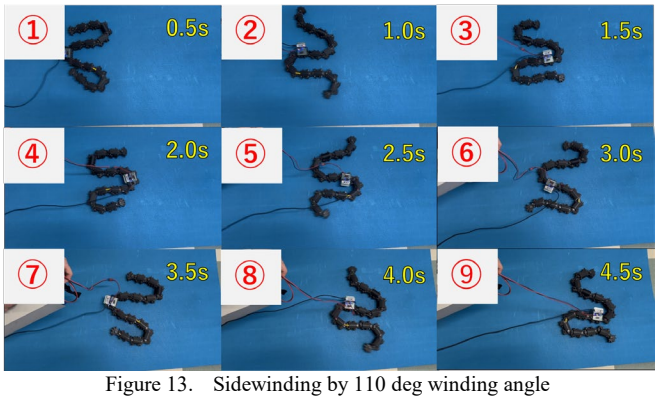

Figure 13. Sidewinding by 110 deg winding angle

V. Experiment and Discussion

Performance experiments were conducted using a prototype to verify movement of sidewinding locomotion. Angular command values for the servomotors are calculated by creating an approximation curve using B-spline interpolation and performing convergence calculations based on Gauss-Green's theorem. Experimental results confirmed that the lifting mechanism raises the body segments, enabling movement on flat surfaces of floor by sidewinding locomotion. Furthermore, the contact point with the ground is a point contact, and since it is constantly sliding in the rotational direction, the friction condition with the floor is dynamic friction. Figure 11 shows the operation at a winding angle of 60 degrees, Figure 12 at 90 degrees, and Figure 13 at 110 degrees. These figures confirm that the body segments bend larger than in previous snake robots, enabling movements closer to those of a real snake.

Analysis of the motion vector determined the direction and distance our snake robot can move. The results of the analysis are shown in Figure 14. The first quadrant of the graph represents movement in the positive direction, while the third quadrant shows movement achieved by reversing the propagation of the angular command value of servomotors. The lifting mechanism of our snake robot exhibits regularity in its bending direction, preventing movement in the directions of the second and fourth quadrants of the graph. If the robot needs to move, it must combine turning actions to achieve the desired movement. The larger the winding angle, the greater the lateral movement. The maximum lateral movement occurs at a winding angle of 90 degrees. When the winding angle exceeds 90 degrees, the component moving along the contact trajectory in the negative y-axis direction becomes positive, allowing for a larger upward movement in the positive y-axis direction. However, when the winding angle exceeds 120 degrees, the body segments come into contact, preventing further increases in angle. When a winding angle is 30 degrees, the positive and negative y-axis displacement components cancel each other out, resulting in a significant reduction in lateral displacement. This analysis clarifies why conventional snake robots have small bending angles and consequently exhibit limited lateral movement.

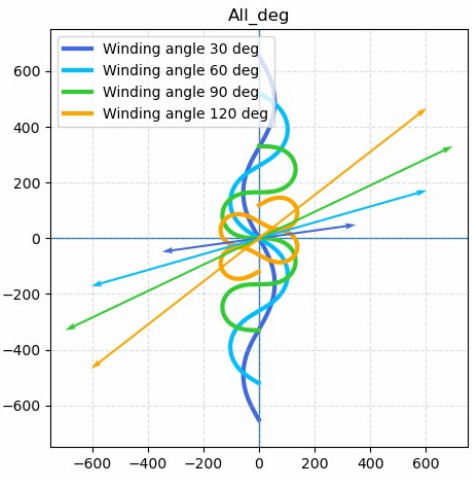

Figure 14. Analysis of the motion vectors of our snake robot can move

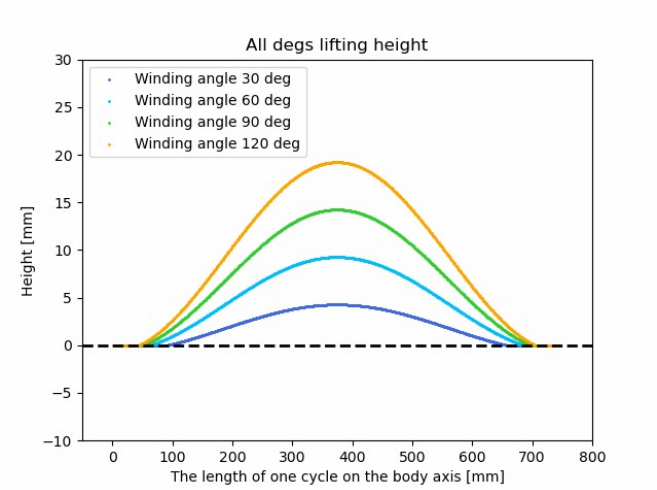

Figure 15. Lifting height per one cycle when varying the winding angle

Figure 15 shows a comparison of the winding angle and body lift amount in our robot. The curves in the graph represent the body lift height per one cycle as the bending angle is varied. Due to the influence of the crossed helical gear mechanism constituting the body segment, the lift amount increases as the horizontal bending becomes larger. Consequently, a larger winding angle results in a greater maximum lifting height. Conversely, a smaller winding angle yields a lower lifting height, and the body cannot lift off the ground due to losses in the lifting mechanism. Therefore, our robot cannot move during sidewinding with a small winding angle.

VI. Conclusion

This study aimed to achieve sidewinding locomotion of the snake robot with reduced degrees of freedom, focusing on the regularity of side-winding. A lifting mechanism using the crossed helical gears was designed, and the mechanisms synchronized with horizontal bending motions to lift the body were developed. Our prototype of snake robot was constructed by connecting the developed the body segments, successfully achieving sidewinding movement. Furthermore, through trajectory planning and analysis of the locomotion, we clarified the characteristics of the sidewinding motion.

In the future work, we plan include implementing trajectory planning that incorporates turning motions to achieve omnidirectional movement.

References

[1] M. Mori and S. Hirose: Three-dimensional serpentine motion and lateral rolling by active cord mechanism ACM-R3, IEEE/RSJ International Conference on Intelligent Robots and Systems, (2002), 829.

[2] C. Wright et al.: Design and architecture of the unified modular snake robot, IEEE International Conference on Robotics and Automation, (2012), 4347.

[3] K. Hoshino, M. Tanaka and F. Matsuno: Optimal shape of a snake robot for jumping, IEEE International Conference on Robotics and Automation, (2010), 697.

[4] K. Suzuki, A. Nakano, G. Endo and S. Hirose: Development of multi-wheeled snake-like rescue robots with active elastic trunk, IEEE/RSJ International Conference on Intelligent Robots and Systems, (2012), 4602.

[5] R. Ariizumi and F. Matsuno: Dynamical analysis of sidewinding locomotion by a snake-like robot, IEEE International Conference on Robotics and Automation, (2013), 5149.

[6] A. H. Chang, M. M. Serrano and P. A. Vela: Shape-centric modeling of lateral undulation and sidewinding gaits for Snake Robots, IEEE 55th Conference on Decision and Control, (2016), 6676.

[7] R. L. Hatton and H. Choset: Sidewinding on slopes, IEEE International Conference on Robotics and Automation, (2010), 691.

[8] M. J. Koopaee, B. Van Huijgevoort, C. Pretty and X. Q. Chen: Parameters tuning of snake robots' sidewinding gait using Bayesian optimization, 4th International Conference on Control, Automation and Robotics, (2018), 43.

[9] M. Mori and S. Hirose: Development of active cord mechanism ACM-R3 with agile 3D mobility, IEEE/RSJ International Conference on Intelligent Robots and Systems, (2001), 1552.

[10] The Amazing Sidewinder: < https://zackandscottkarmachameleons. wordpress.com/2016/03/04/the-amazing-sidew inder/>, (accessed 2025-08-30).

[11] Y. Naito., K. Nakano. And T. Aoki. “Snake Robot for Sidewinding Movement,” JSME ROBOMECH, (2022), 2A2-T09, (in Japanese).

[12] T. AOKI., K. NAKANO. and Y. NAGANO. "Development of Lift Up Mechanism for Sidewinding Locomotion of Snake Robot," Proc. of The 6th International Conference on Design Engineering and Science, pp296-305, 2025

[13] S. Hirose, Biologically Inspired Robots (Snake-like Locomotor andManipulator). Oxford University Press, 1993.